eLIFE elifesciences.org

RESEARCH ARTICLE

Figures and figure supplements

Targeting of the Fun30 nucleosome remodeller by the Dpb11 scaffold facilitates cell cycle-regulated DNA end resection

Susanne CS Bantele *et al*

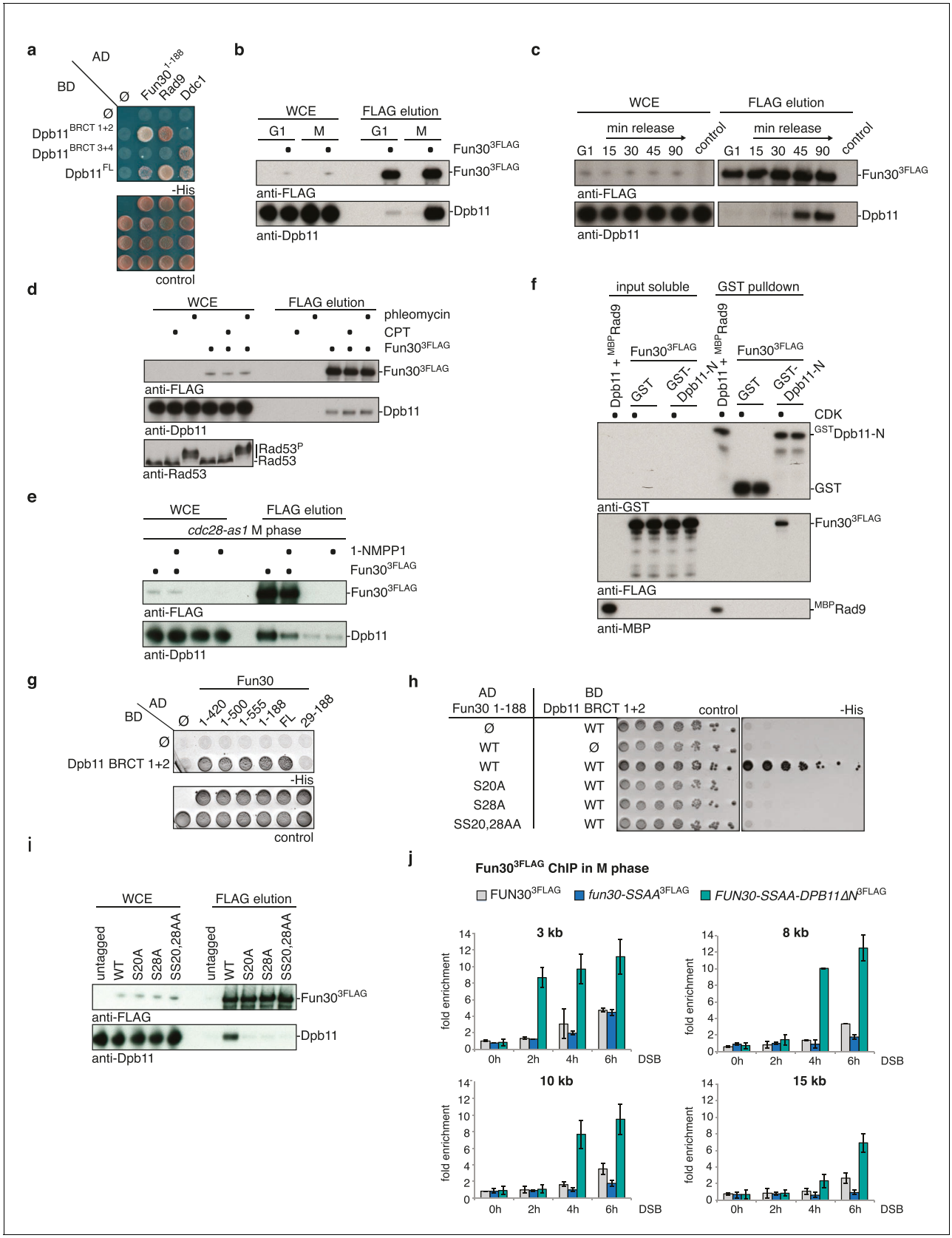

Figure 1. Fun30 and Dpb11 interact in a cell cycle- and CDK phosphorylation-dependent manner and this targets Fun30 to DSBs. (**a**) Two-hybrid assay with GAL4-AD and -BD constructs as indicated reveals a physical interaction between the N-terminal region of Fun30 (aa 1–188) and the BRCT1+2

Figure 1 continued on next page

Figure 1 continued

domain of Dpb11. Rad9 and Ddc1 represent known interactors of BRCT1+2 and BRCT3+4, respectively. (**b–e**) Characterization of the Fun30-Dpb11 interaction by Fun30^{3FLAG} Co-IP experiments. Dpb11 was expressed from the strong, constitutive GPD promoter. (**b**) Fun30^{3FLAG} specifically binds Dpb11 in cells arrested in M but not G1 phase. (**c**) Fun30^{3FLAG} purified from cells synchronously progressing through the cell cycle binds Dpb11 only at 45' and 90' time points corresponding to late S and M phase (***Figure 1—figure supplement 2*** for FACS analysis and western analysis of cell cycle progression). (**d**) No enhancement of the Fun30-Dpb11 interaction by CPT or phleomycin treatment as measured by Fun30^{3FLAG} Co-IP. For DNA damage treatment, 50 µM CPT or 50 µg/ml phleomycin were added to asynchronously dividing yeast cells. DNA damage checkpoint activation was measured by Rad53 phosphorylation in IP extracts (lowest blot panel). (**e**) CDK inhibition using the *cdc28-as1* allele and 1-NMPP1 treatment diminishes the Fun30^{3FLAG}-Dpb11 interaction in M phase arrested cells. (**f**) Purified Fun30 interacts with a BRCT1+2 fragment of Dpb11 in the presence of CDK phosphorylation. Purified Fun30^{3FLAG} or the positive control ^{MBP}Rad9 (***Pfander and Diffley, 2011***) were incubated with a model CDK and ATP before binding to bead-bound ^{GST}Dpb11 BRCT1+2. (**g**) Mapping analysis of the two-hybrid interaction between Fun30 and Dpb11 reveals a binding site close to the N-terminus of Fun30. (**h–i**) Putative CDK sites on Fun30 (S20 and S28) are required for Dpb11 binding. (**h**) Two-hybrid assay as in (**a**) but in five-fold serial dilution and with *WT*, *S20A*, *S28A* and *SS20,28AA* variants of Gal4-AD-Fun30$^{1-188}$. (**i**) Co-IP as in (**b**) but with mutant variants of Fun30^{3FLAG} growing asynchronously. (**j**) Efficient Fun30 localization to damaged chromatin requires the Dpb11-Fun30 interaction. ChIP of Fun30^{3FLAG} to chromatin locations 3, 8, 10 and 15 kb distant of a non-repairable DSB induced at the MAT locus in M phase-arrested cells. *fun30* mutants were expressed from the endogenous promoter as only copy of *FUN30*. The *FUN30-DPB11* fusion contains *fun30-SSAA* and *dpb11△N* mutations. *WT*, *fun30-SSAA* and *FUN30-DPB11 fusion* cells were crosslinked at indicated timepoints after DSB induction. Plotted values represent means from two independent experiments, error bars represent standard deviations.

DOI: 10.7554/eLife.21687.003

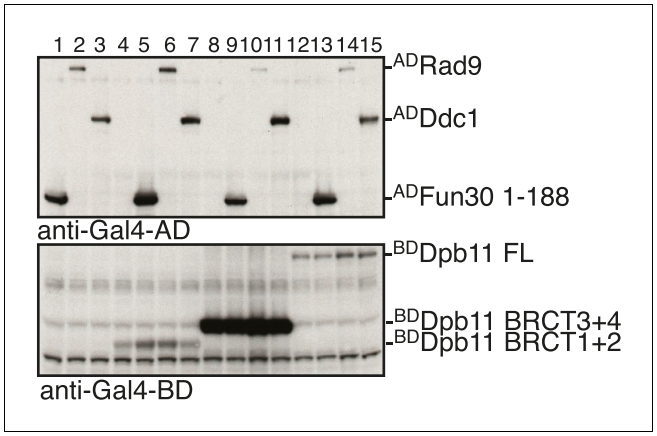

Figure 1—figure supplement 1. Expression control of two-hybrid constructs used in ***Figure 1A***. Two-hybrid constructs are detected with anti-Gal4-AD (AD-Fun30 1–188, AD-Ddc1, AD-Rad9) and with anti-Gal4-BD (for BD-Dpb11 constructs) antibodies.
DOI: 10.7554/eLife.21687.004

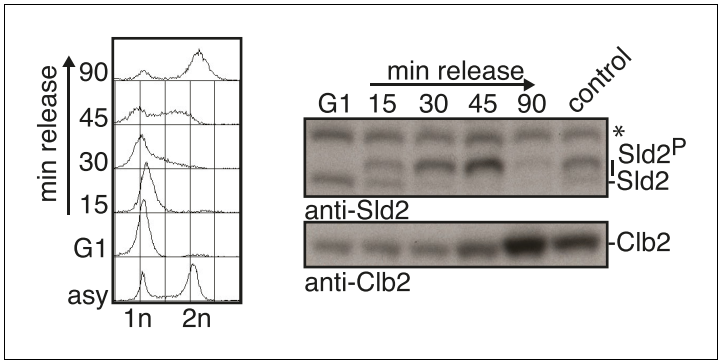

Figure 1—figure supplement 2. Control of the cell cycle states of the experiment in ***Figure 1C***. Left panel: DNA content measurements with FACS. Right panel: Western Blot analysis using S/M-phase (hyperphosphorylated Sld2) or M-phase (Clb2) markers. Asterisk indicates a cross reactive band.
DOI: 10.7554/eLife.21687.005

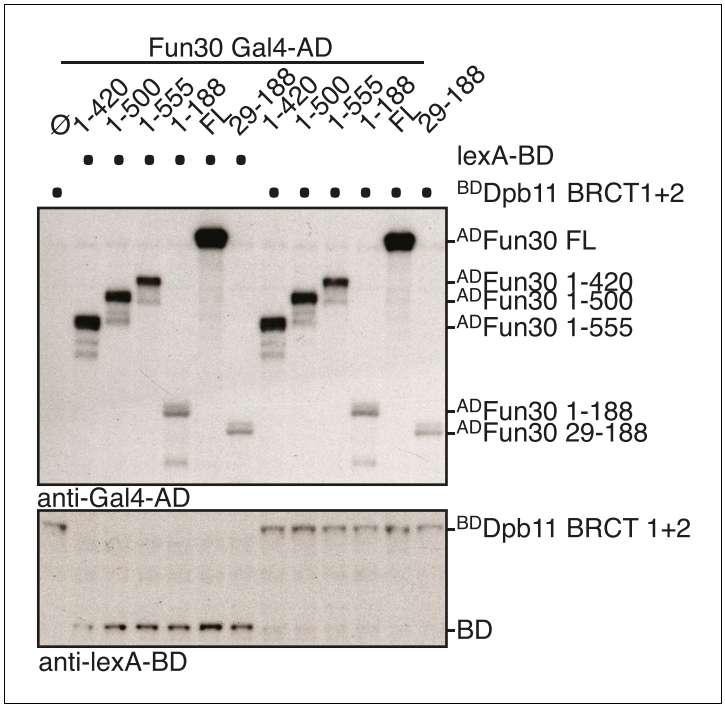

Figure 1—figure supplement 3. Expression control of two-hybrid constructs used in ***Figure 1G***. Two-hybrid constructs are detected with anti-Gal4-AD (AD-Fun30 constructs) and with anti-lexA-BD (for BD-Dpb11 BRCT1 +2 construct) antibodies.

DOI: 10.7554/eLife.21687.006

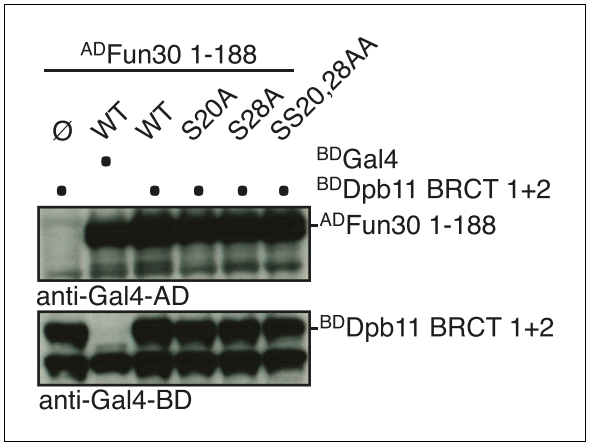

Figure 1—figure supplement 4. Expression control of two-hybrid constructs used in ***Figure 1H***. Two-hybrid constructs are detected with anti-Gal4-AD (AD-Fun30 1–188 and mutant derivatives) and with anti-Gal4-BD (for BD-Dpb11 BRCT1 +2 constructs) antibodies.
DOI: 10.7554/eLife.21687.007

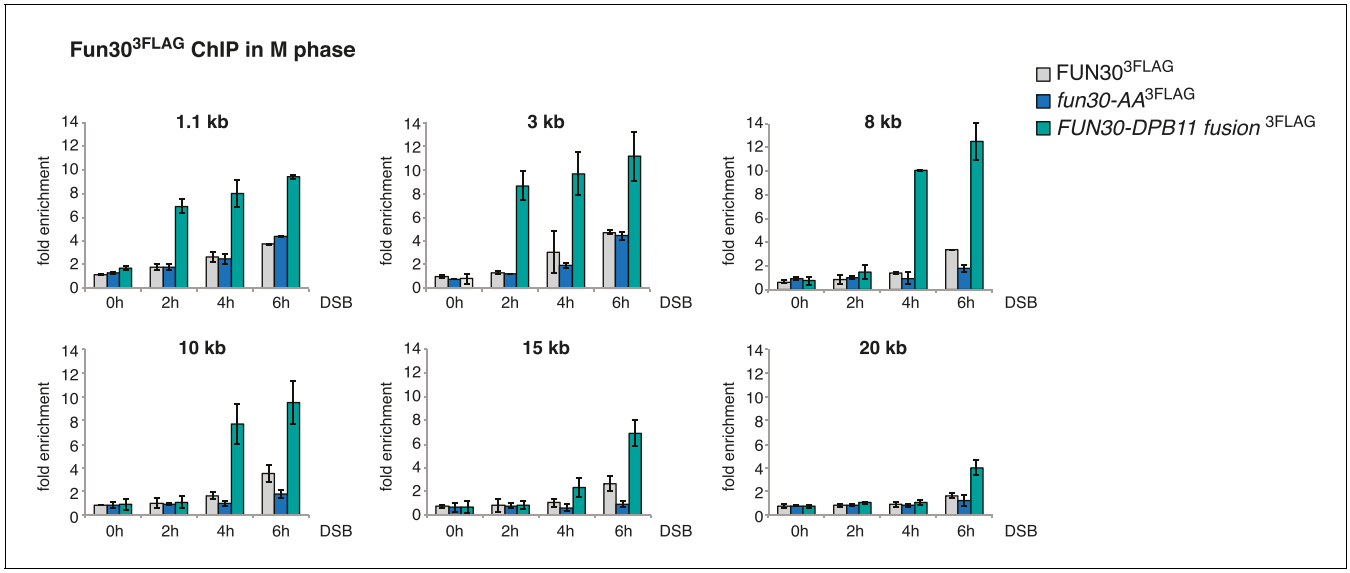

Figure 1—figure supplement 5. Efficient Fun30 localization to damaged chromatin requires the Dpb11-Fun30 interaction. ChIP of Fun30^{3FLAG} to chromatin in proximity of a non-repairable DSB induced at the MAT locus in M phase arrested cells. Same experiment as in ***Figure 1J***, using *WT*, *fun30-SSAA* and *FUN30-DPB11 fusion* cells, but here Fun30 ChIP is shown at additional loci (1.1, 3, 8, 10, 15 and 20 kb distance from break). Cells were crosslinked at distinct time points after DSB induction. Plotted values represent error bars from three independent experiments.
DOI: 10.7554/eLife.21687.008

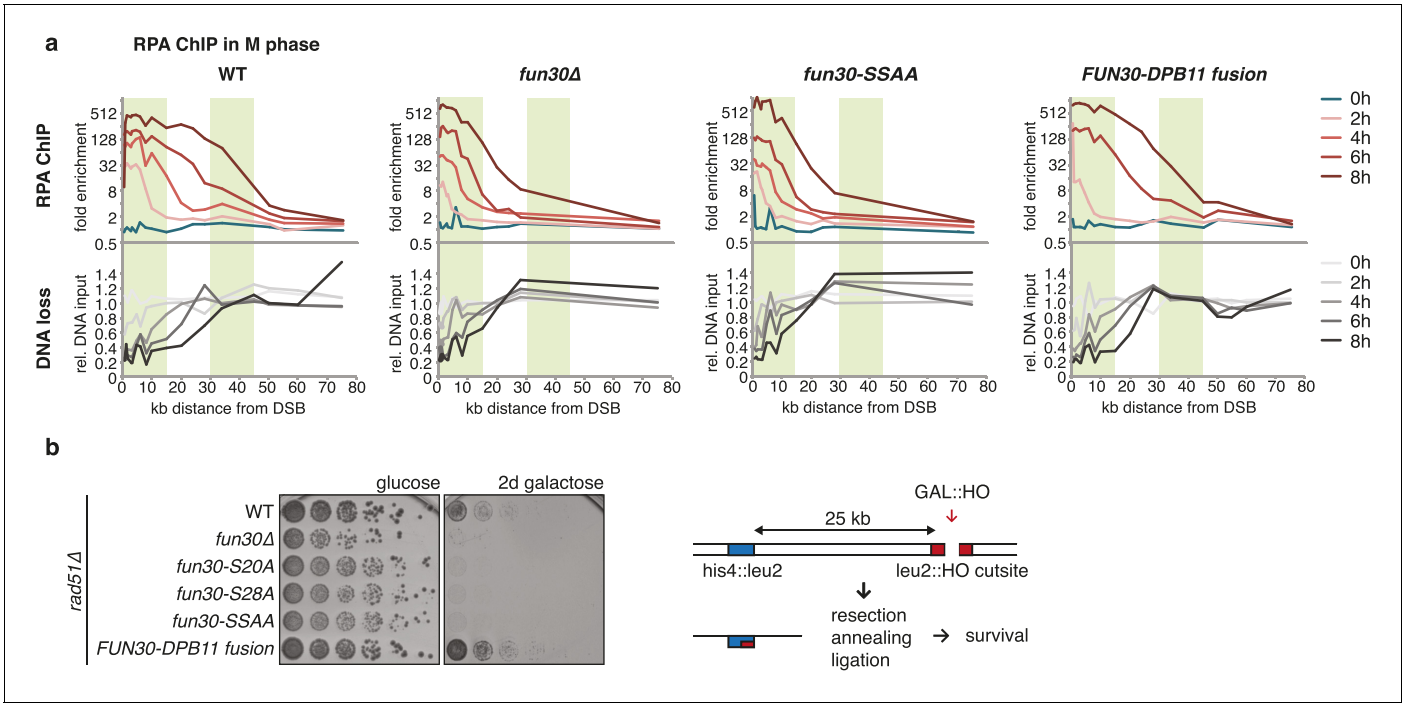

Figure 2. The Fun30-Dpb11 complex is required for efficient long-range resection. (**a**) Long-range resection of a DSB is dependent on the Fun30-Dpb11 interaction. A non-repairable DSB at MAT was induced in M phase-arrested *WT*, *fun30*△, *fun30-SSAA* and *FUN30-DPB11* fusion strains and DNA end resection measured at indicated times. Upper panel: fold enrichment of a given locus in an RPA ChIP relative to undamaged control loci. Lower panel: DNA loss relative to control loci located in non-damaged chromatin. (**b**) Single-strand annealing (SSA) is dependent on the Fun30-Dpb11 interaction. *FUN30* mutants as indicated were combined with the *rad51*△ deletion, a DSB at the leu2::HO cutsite was induced by plating cells on galactose. Cells need to resect 25 kb up to the homologous his4::leu2 locus in order to survive by SSA.

DOI: 10.7554/eLife.21687.009

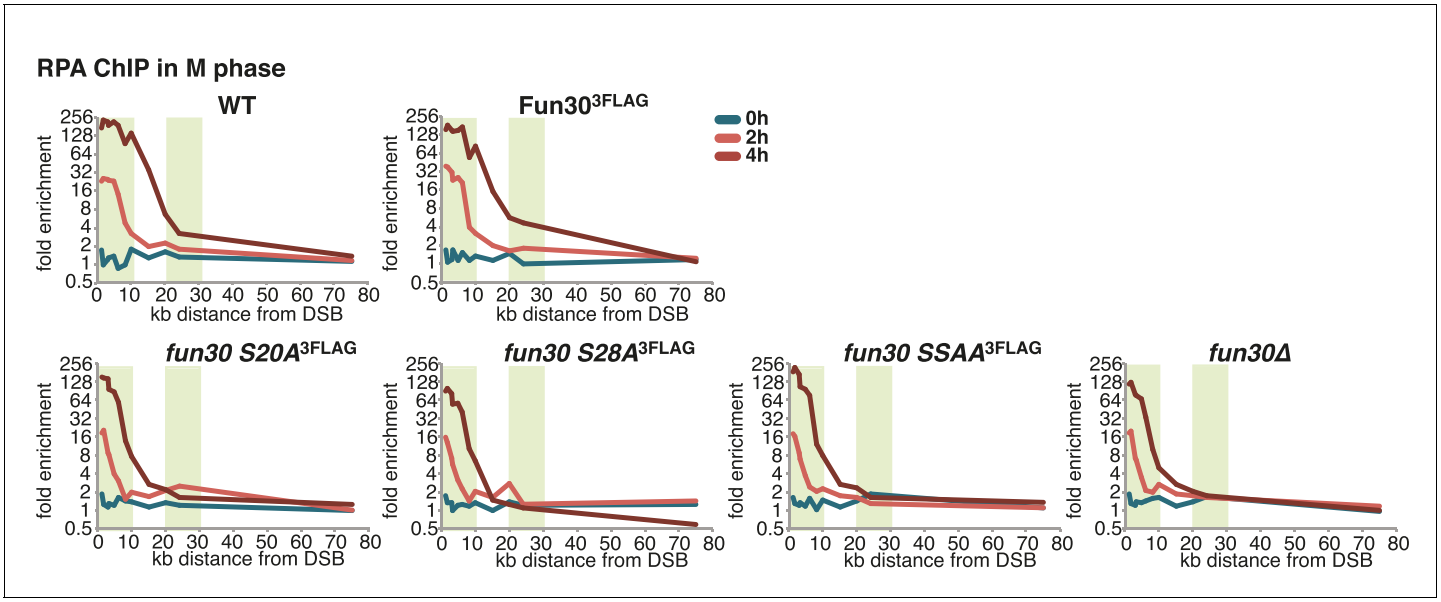

Figure 2—figure supplement 1. The Fun30-Dpb11 interaction is required for efficient long-range resection. Long-range resection of a site-specific DSB is partially deficient in CDK-phosphorylation site mutants that are deficient in the Fun30-Dpb11 interaction. A non-repairable DSB at MAT was induced in M-phase arrested *WT*, *fun30-S20A*^{3FLAG}, *fun30-S28A*^{3FLAG}, *fun30-SSAA*^{3FLAG} and *fun30*Δ cells. DNA end resection was measured at indicated time points by RPA ChIP. Plotted is the fold enrichment of a given locus relative to three undamaged control loci.

DOI: 10.7554/eLife.21687.010

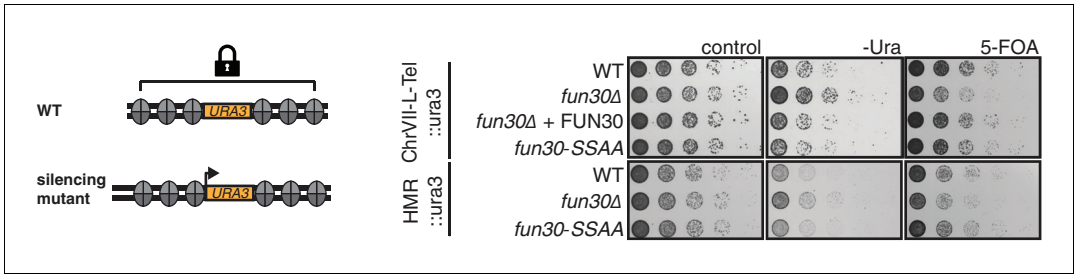

Figure 3. The Fun30-Dpb11 interaction is not involved in Fun30-dependent gene silencing at telomeric heterochromatin and a silent mating type locus. The silencing defect of the *fun30Δ* mutant is not recapitulated by the *fun30-SSAA* mutant. Two silencing tester strains were used: the first (upper panels) had URA3 integrated in telomeric heterochromatin at the end of the left arm of chromosome VII, the second (lower panels) had URA3 integrated at the HML silent mating type locus. A silencing defect leads to enhanced growth on –Ura medium and less growth on medium supplemented with 5-FOA (e.g. *fun30Δ*). Shown is a spotting in 5-fold serial dilutions on non-selective medium, medium lacking uracil or containing 5-FOA.

DOI: 10.7554/eLife.21687.011

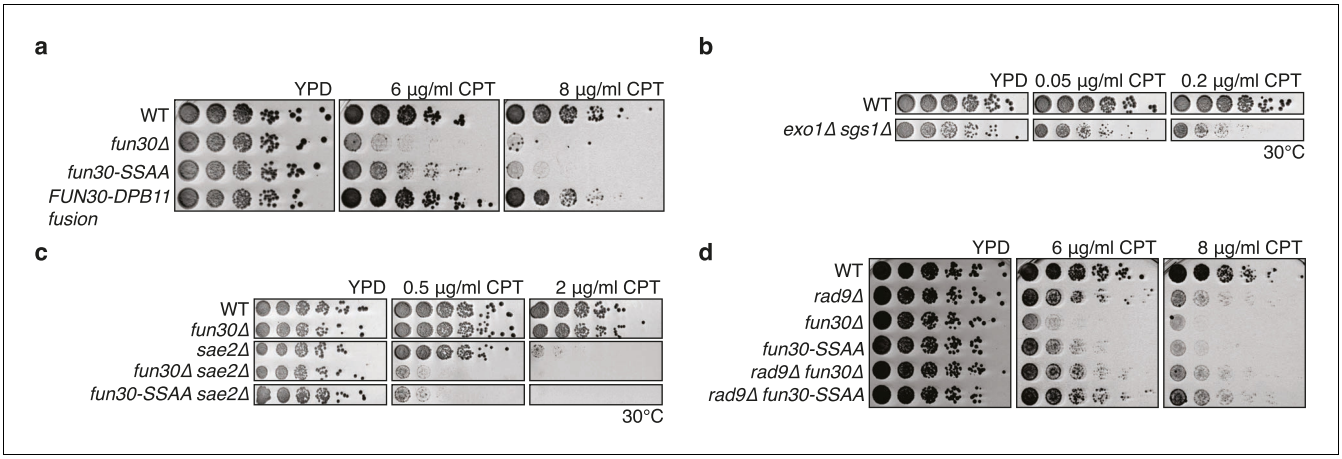

Figure 4. The Fun30-Dpb11 interaction is required for the response towards CPT, as is functional long- and short-range resection. (**a**) The Fun30-Dpb11 interaction is required for the response towards CPT. *WT*, *fun30△*, *fun30-SSAA* and *FUN30-DPB11 fusion* were spotted in five-fold serial dilutions on plates containing indicated amounts of CPT and incubated at 37˚C for two days. (**b**) A double mutant of *exo1Δ* and *sgs1Δ* is hyper-sensitive to low doses of CPT. Spotting in 5-fold serial dilutions was incubated for two days at 30˚C. (**c**) The *fun30Δ/fun30-SSAA* mutants enhance the CPT hyper-sensitivity of *sae2Δ* mutants. Cells were spotted in 5-fold serial dilutions and incubated for two days at 30˚C. (**d**) A *rad9Δ* deletion rescues CPT hyper-sensitivity of *fun30Δ* and *fun30-SSAA* mutant alleles.

DOI: 10.7554/eLife.21687.012

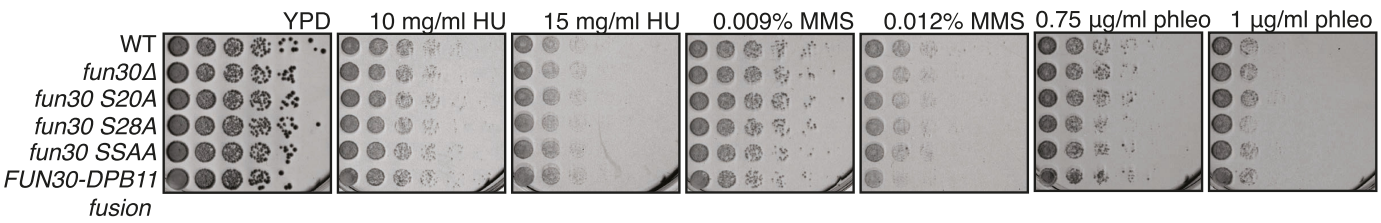

Figure 4—figure supplement 1. Mutants of Fun30 show no discernable phenotype upon chronic exposure to HU, MMS or phleomycin. Spotting in 5-fold serial dilutions on medium containing indicated dosages of DNA damaging agents. Plates were incubated two days at 30°C.
DOI: 10.7554/eLife.21687.013

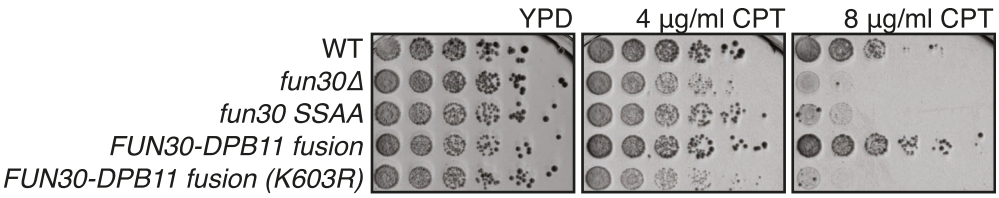

Figure 4—figure supplement 2. The catalytic activity of Fun30 is required for the suppression of the CPT phenotype in the context of the *FUN30-DPB11 fusion*. Spotting of strains with indicated genotypes in 5-fold serial dilutions on CPT containing medium. The K603R mutation is located in the Walker A motif of Fun30. Plates were incubated for two days at 37°C.

DOI: 10.7554/eLife.21687.014

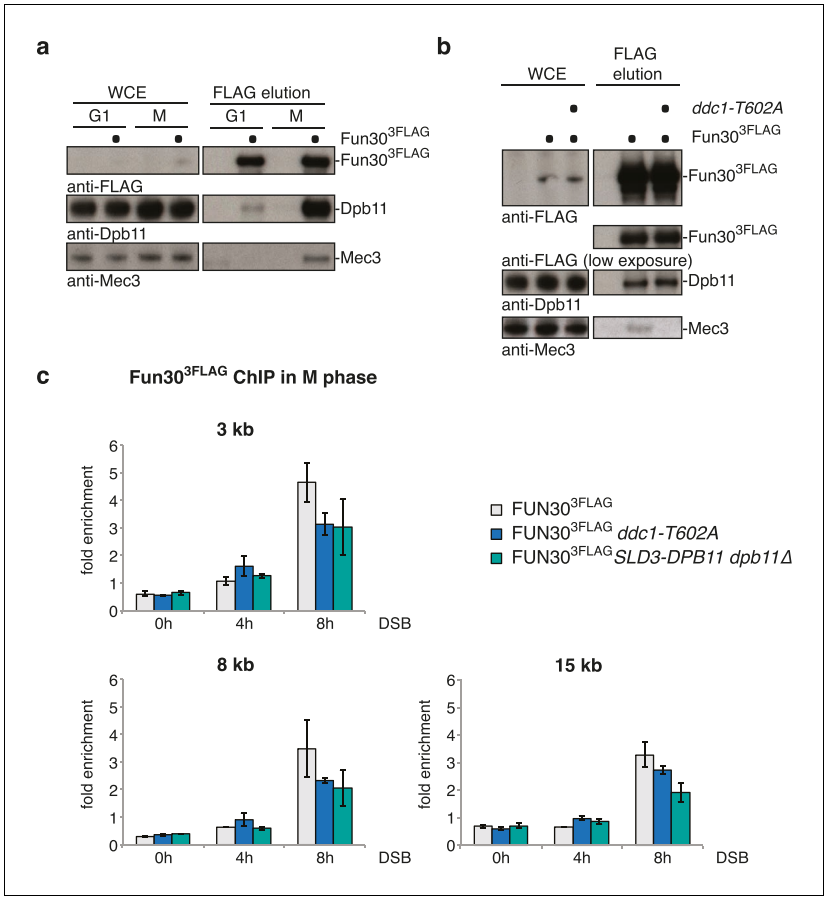

Figure 5. The 9-1-1 complex forms a ternary complex with Fun30-Dpb11. (**a**) Fun30, Dpb11 and 9-1-1 form a ternary complex. The 9-1-1 subunit Mec3 interacts with Fun30^{3FLAG} when purified from M phase cells, where also Dpb11 binds to Fun30. (**b**) The *ddc1-T602A* mutation abolishes binding of Mec3 to Fun30-Dpb11 in Fun30^{3FLAG} Co-IPs, but leaves the Fun30-Dpb11 interaction intact. (**c**) Mutants disrupting the interaction between 9-1-1 and Dpb11 (*ddc1-T602A*) or Fun30 and Dpb11 (*SLD3-dpb11ΔN*, lacks Fun30 binding site, only copy of Dpb11) impair efficient localization of Fun30 to DSBs in Fun30^{3FLAG} ChIPs of M phase-arrested cells. Experiment performed as in ***Figure 1J***, plotted values represent means of two independent experiments, error bars represent standard deviations.

DOI: 10.7554/eLife.21687.015

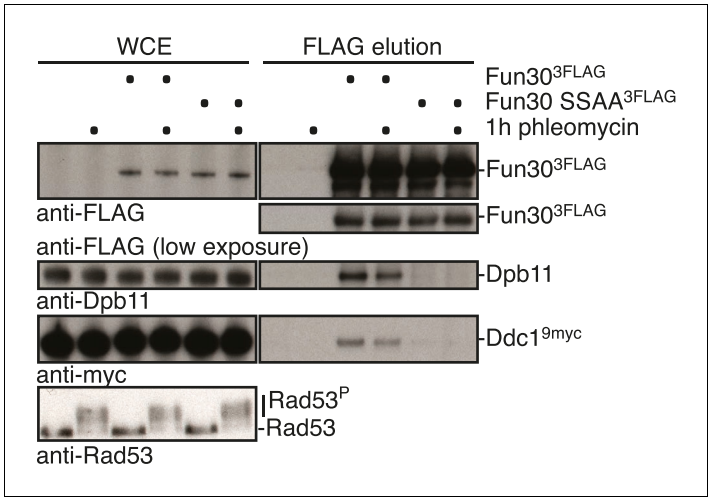

Figure 5—figure supplement 1. The interaction between Fun30 and 9-1-1 depends on mutual interactions with Dpb11, suggesting that Dpb11 forms a molecular bridge in the Fun30-Dpb11-9-1-1 complex. The *fun30-SSAA* mutation abolishes binding of Dpb11 and also Ddc1^{9myc} in Fun30^{3FLAG} Co-IPs. Cells were either left untreated or treated with 50 µg/ml phleomycin, which induced the DNA damage checkpoint (Rad53 activation), but did not influence Dpb11 or Ddc1 binding.

DOI: 10.7554/eLife.21687.016

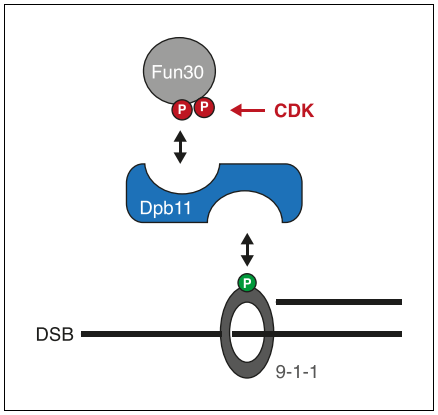

Figure 5—figure supplement 2. Model of the Fun30-Dpb11-9-1-1 association and its regulation.
DOI: 10.7554/eLife.21687.017

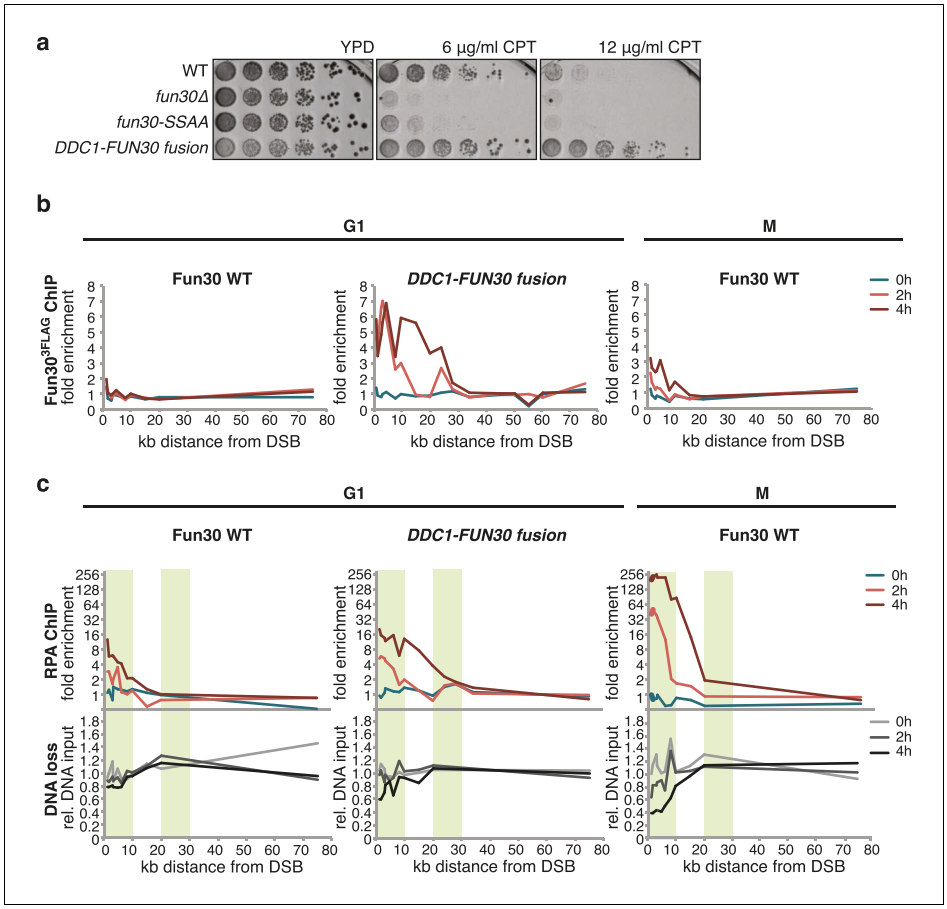

Figure 6. A covalent fusion of Fun30 to the 9-1-1 subunit Ddc1 generates a bypass of the cell cycle regulation of long-range resection. (**a**) The *DDC1-FUN30* fusion confers cellular hyper-resistance to CPT. Spotting of indicated strains as in ***Figure 4A***, but using CPT concentrations of up to 12 µg/ml. (**b**) The *DDC1-FUN30* fusion localizes efficiently to a DSB in G1-arrested cells. Fun30^{3FLAG} ChIPs from *WT*, *fun30-SSAA*, *FUN30-DPB11* and *DDC1-FUN30* cells as in ***Figure 1J***, but from G1 or M phase-arrested cells. Additional Fun30^{3FLAG} ChIP data can be found in ***Figure 6—figure supplement 3***. (**c**) The *DDC1-FUN30* fusion enhances long-range resection in G1-arrested cells. Resection assay as in ***Figure 2A***, but with G1 or M phase-arrested cells. Additional resection assay data can be found in ***Figure 6—figure supplement 3***.

DOI: 10.7554/eLife.21687.018

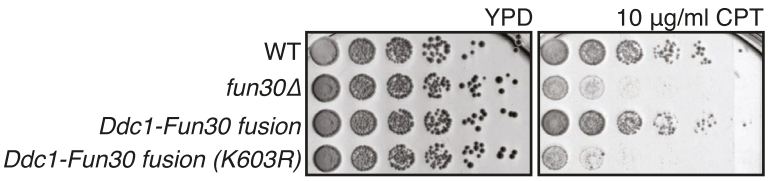

Figure 6—figure supplement 1. The *DDC1-FUN30 fusion* rescues the CPT sensitivity of the *fun30△* mutant in a manner that depends on the Fun30 catalytic activity. *WT*, *fun30Δ*, *DDC1-FUN30 fusion* and *DDC1-FUN30 (K603R) fusion* mutants are spotted on CPT as in ***Figure 4A***.

DOI: 10.7554/eLife.21687.019

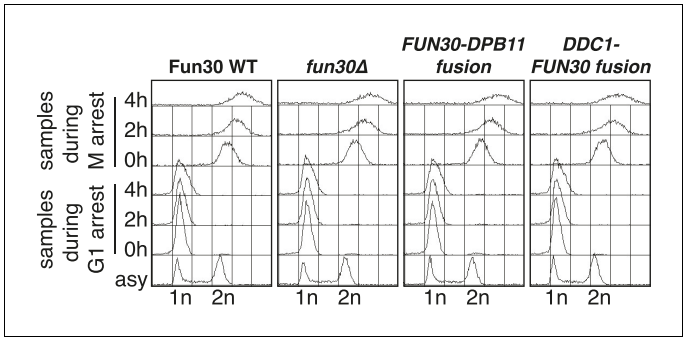

Figure 6—figure supplement 2. Flow cytometric analysis of DNA content for experiments shown in ***Figure 6B–C*** and ***Figure 6—figure supplement 3***.

DOI: 10.7554/eLife.21687.020

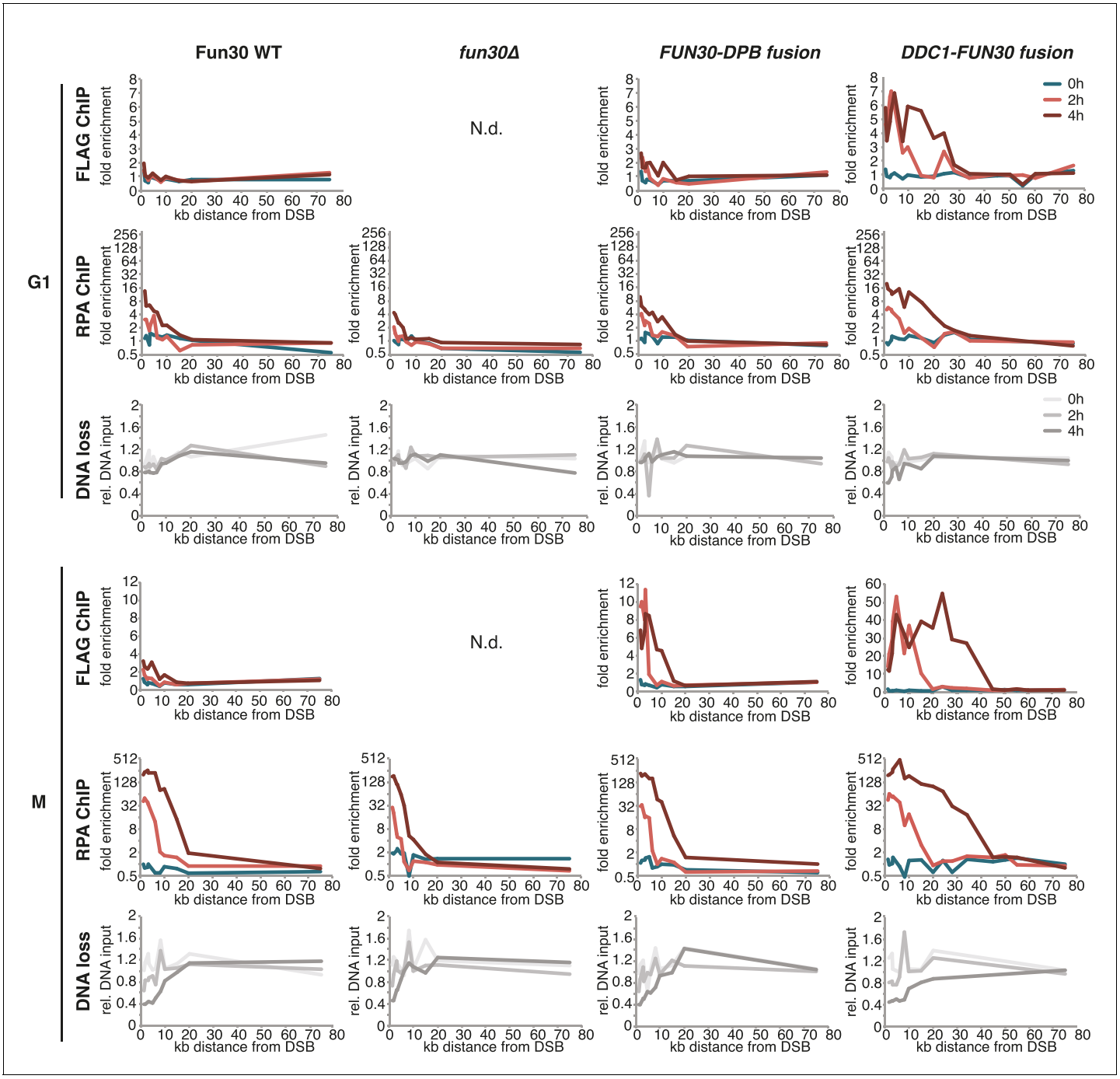

Figure 6—figure supplement 3. The *DDC1-FUN30 fusion* protein efficiently localizes to DSBs and promotes hyper-resection in M phase as well as allowing long-range resection in G1 phase. Cells (*WT, fun30Δ and DDC1-FUN30 fusion*) were arrested in G1 or M phase prior to DSB induction. Fun30 localization was investigated by anti-FLAG ChIP after break induction (upper panels). DNA end resection was investigated by the combined read-out of RPA ChIP and DNA loss (lower panels).

DOI: 10.7554/eLife.21687.021

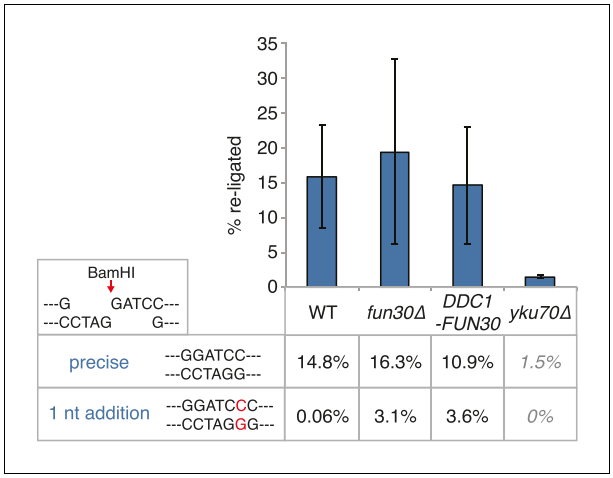

Figure 7. The *DDC1-FUN30* fusion does not significantly inhibit non-homologous end-joining (NHEJ). Precise re-ligation of BamHI-cut pRS316 as measured by cell viability on SC-Ura plates and subsequent sequencing of single colonies was dependent on Ku70 but not significantly affected in *DDC1-FUN30* of *fun30*Δ mutant cells. Plotted are values from three independent experiments representing the viability rate of cells on SC-Ura plates relative to the total cell number and the transformation efficiency of the mock-digested plasmid. Error bars represent standard deviations.

DOI: 10.7554/eLife.21687.022

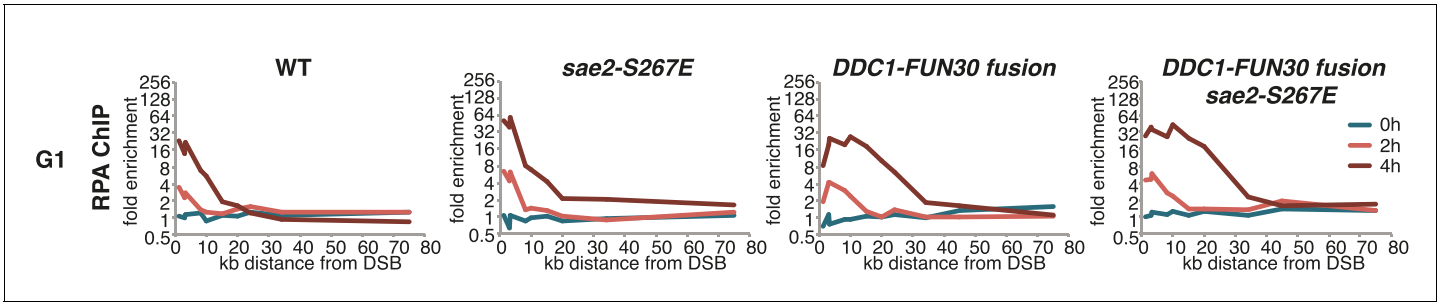

Figure 8. The *DDC1-FUN30* fusion specifically enhances long-range resection in G1, while the *sae2-S267E* phospho-mimicry leads to a small increase in resection initiation. The *sae2-S267E* mutant has little effect on the spreading of DNA end resection in G1, but slightly stimulates the RPA fold enrichment in *WT* and the *DDC1-FUN30* fusion mutant. This suggests that *sae2-S267E* in contrast to the *DDC1-FUN30* fusion does not affect long-range resection. DNA end resection in the indicated strains was analysed by RPA ChIP as in ***Figure 5C*** but with G1 arrested cells.
DOI: 10.7554/eLife.21687.023

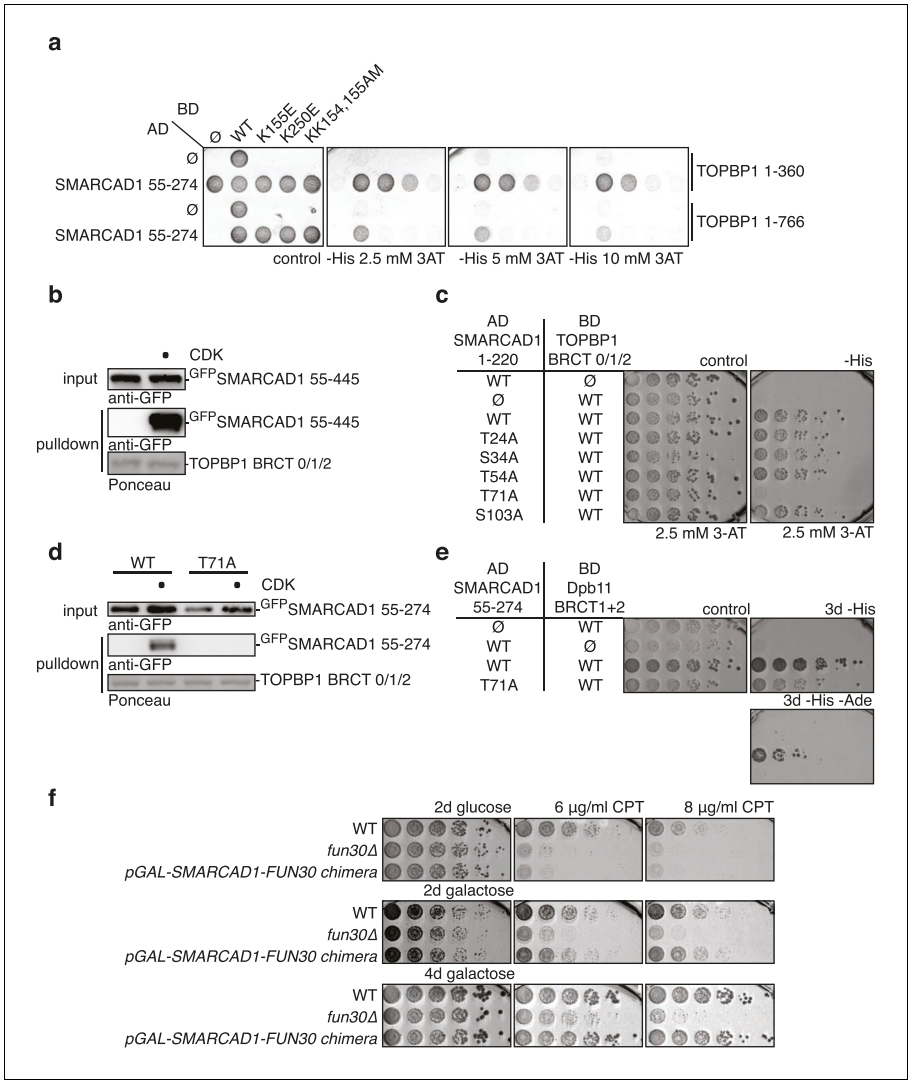

Figure 9. Yeast Fun30 and human SMARCAD1 underlie a conserved regulation. (**a**) SMARCAD1 and TOPBP1 interact and their interaction depends on functional phospho-binding pockets in BRCT1 and BRCT2 of TOPBP1. lexA-BD TOPBP1 1–360 (harbouring BRCT0/1/2) or lexA-BD TOPBP1 1–766 (harbouring BRCT0-5) were tested as *WT* versions or as *K155E, KK154,155AM* (affecting BRCT1) or *K250E* (affecting BRCT2) mutant derivatives. Interaction was tested against the Gal4-AD SMARCAD1 55–274. 3AT was added to –His plates to suppress auto-activation and to increase the stringency of the two-hybrid. Two-hybrid interactions with the lexA-BD TOPBP1 1–360 construct were generally stronger compared to lexA-BD TOPBP1 1–766, leading to milder effects of the K155E and K250E single-mutants, particularly at low 3AT concentrations. (**b**) SMARCAD1 interacts with TOPBP1 after CDK phosphorylation. ^{GFP}SMARCAD1 (55-445) was bound to a ^{GST}TOPBP1 BRCT0/1/2 construct after phosphorylation with CDK. This CDK-dependent interaction was seen with several N-terminal SMARCAD1 constructs, but not with FL, perhaps due to low expression. (**c–d**) Threonine 71 of SMARCAD1, a putative CDK phosphorylation site, is required for TOPBP1 binding. (**c**) Two-hybrid analysis of ^{AD}SMARCAD1 (1-220) and phospho-mutant derivatives to ^{BD}TOPBP1 BRCT0/1/2. (**d**) Co-IP as in (**a**), but additionally using a T71A variant of ^{GFP}SMARCAD1 (55-274). (**e**) Dpb11 can bind to human SMARCAD1, and T71 is important for the interaction. Two-hybrid analysis as in (**b**), but using a ^{BD}Dpb11 BRCT1+2 construct. (**f**) A SMARCAD1-Fun30 chimera lacking the Dpb11-binding site of Fun30, but containing the TOPBP1-binding site of SMARCAD1 restores sensitivity to CPT. The SMARCAD1-Fun30 chimera is expressed from the pGAL1-10 promoter and induced by galactose. Spotting on CPT medium as in ***Figure 4A***.
DOI: 10.7554/eLife.21687.024

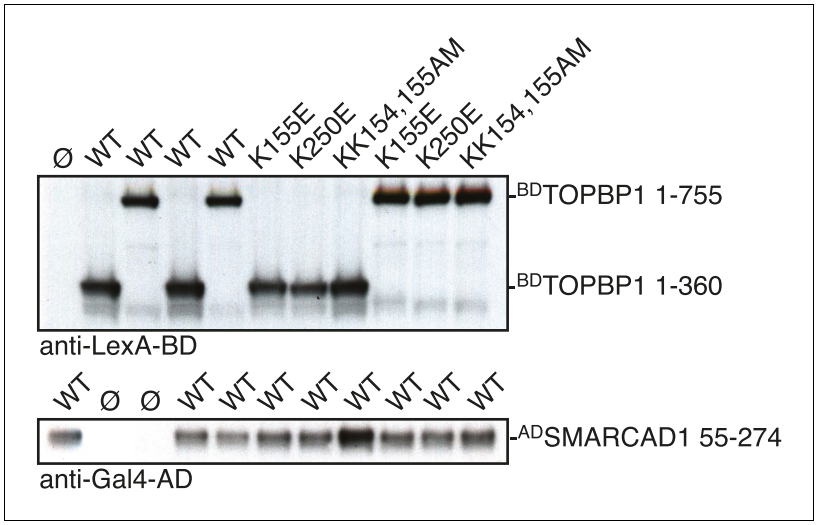

Figure 9—figure supplement 1. The interaction between SMARCAD1 and TOPBP1 depends on functional phospho-binding pockets in BRCT1 and 2 of TOPBP1. Expression control for two-hybrid constructs in ***Figure 9A*** using anti-lexA-BD and anti-Gal4-AD antibodies.
DOI: 10.7554/eLife.21687.025

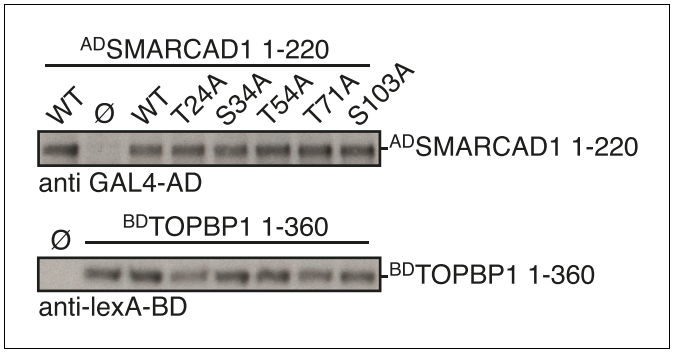

Figure 9—figure supplement 2. Threonine 71 of SMARCAD1, a putative CDK phosphorylation site, is required for TOPBP1 binding. Expression control for two-hybrid constructs in ***Figure 9C*** using anti-lexA-BD and anti-Gal4-AD antibodies.

DOI: 10.7554/eLife.21687.026

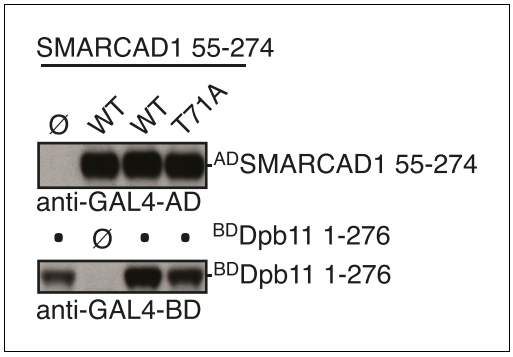

Figure 9—figure supplement 3. Dpb11 can bind to human SMARCAD1, and T71 is important for the interaction. Expression control for two-hybrid constructs in ***Figure 9E*** using anti-Gal4-BD and anti-Gal4-AD antibodies.
DOI: 10.7554/eLife.21687.027

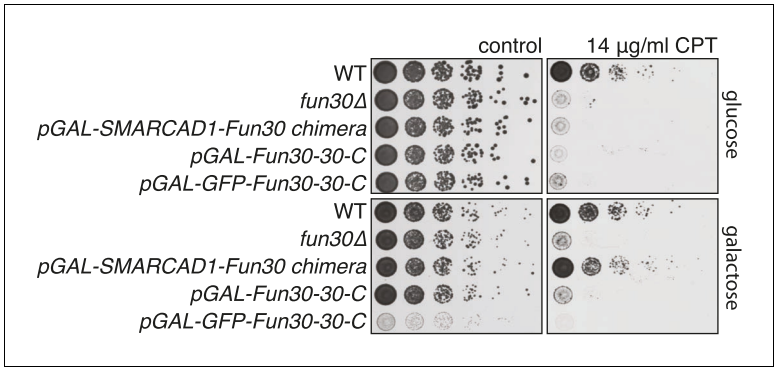

Figure 9—figure supplement 4. A SMARCAD-FUN30 chimera lacking the Dpb11 binding site of Fun30 but containing the putative TOPBP1 binding site of SMARCAD1 restores sensitivity to CPT, while expression of the Fun30 construct lacking the Dpb11 binding site does not. The SMARCAD1-FUN30 chimera, FUN30 30–C and GFP-FUN30 30–C constructs are expressed from the pGAL1-10 promoter and induced by galactose. Spotting on CPT medium as in ***Figure 4A***.

DOI: 10.7554/eLife.21687.028

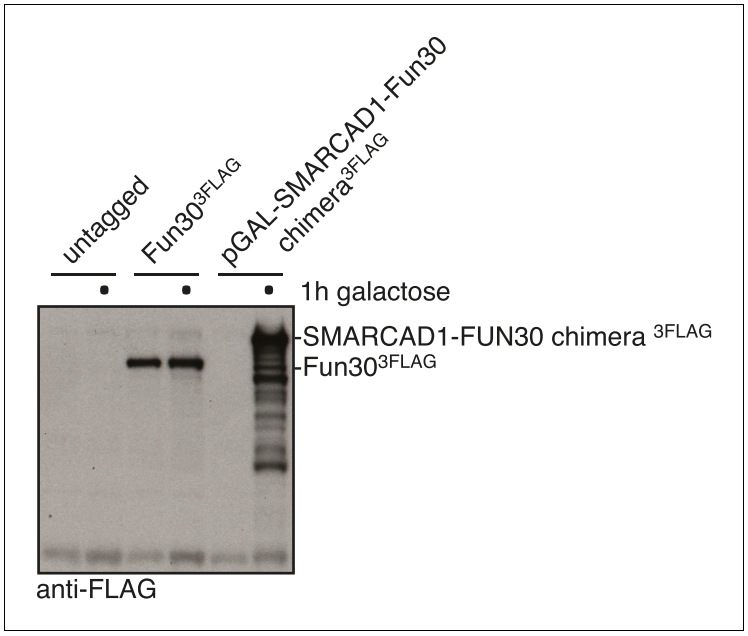

Figure 9—figure supplement 5. Expression control of the SMARCAD1-FUN30 chimera in ***Figure 9F***. SMARCAD1-FUN30 ^{3FLAG} chimerais expressed from the GAL1-10 promoter by addition of galactose. Fun30 ^{3FLAG} expressed from the endogenous promoter serves as control to visualize expression levels of the chimera.
DOI: 10.7554/eLife.21687.029

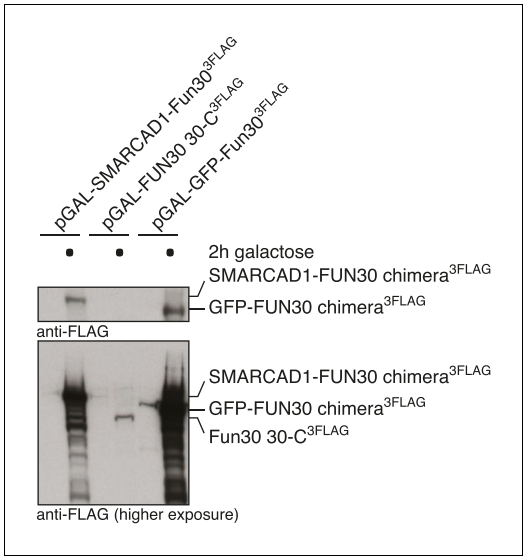

Figure 9—figure supplement 6. Expression control of the SMARCAD1-FUN30 chimera, FUN30-30-C and GFP-FUN30 30-C in ***Figure 9—figure supplement 4*** . SMARCAD1-FUN30^{3FLAG} chimera, FUN30-30-C and GFP-FUN30 30 C are expressed from the GAL1-10 promoter by addition of galactose, which however leads to a stronger expression of the chimera constructs than the truncated FUN30 fragment alone.
DOI: 10.7554/eLife.21687.030